J. Fluid Mech. (1990), *vol.* 213, *pp.* 11–20
Printed in Great Britain

Biofluiddynamics of balistiform and gymnotiform locomotion. Part 3. Momentum enhancement in the presence of a body of elliptic cross-section

By JAMES LIGHTHILL
Department of Mathematics, University College, Gower Street, London WC1E 6BT, UK

(Received 29 March 1989)

Cross-sectional shapes of many fish bodies are well approximated by ellipses. The simple elongated-body theory of balistiform locomotion was developed by Lighthill & Blake (1990) only in the limiting case when the axis ratio of the cross-section tends to zero. In that case they established that the movements of dorsal and anal fins, if attached to a rigid fish body of far greater depth, create fluid motions with substantially enhanced momentum. In this paper, standard conformal mappings are used to establish that enhancement is substantial also with elliptic cross-sections of arbitrary axis ratio, not only in balistiform locomotion with synchronous movement of two median fins but also in gymnotiform locomotion with movement of just a single (ventral) fin.

1. Introduction

For the biological background to this analysis see Lighthill & Blake (1990, hereafter referred to as Part 1). The present paper calculates the fluid momentum associated with a precisely two-dimensional motion resulting from non-uniform movement of a fin (e.g. a rotation about the base), or of a pair of fins, attached to a body of elliptic cross-section. In either case the calculated momentum is compared with the momentum of the fin or fins 'by themselves'.

As regards a single fin by itself, stretched between (say) $x = A$ and $x = B$ (see figure 1) on the axis $y = 0$, where the y-component of velocity of the fin takes the value $f(x)$, the corresponding y-component of momentum takes the form

$$M = 2\rho \int_A^B f(x)\,(x-A)^{\frac{1}{2}}(B-x)^{\frac{1}{2}}\,\mathrm{d}x, \tag{1}$$

where ρ is the fluid density. This result (1) will be recognized as an immediate generalization of the result proved in §4 of Part 1 and there numbered equation (10).

In the familiar case of uniform motion, with $f(x)$ taking the constant value U, equation (1) yields the classical conclusion

$$M = \tfrac{1}{4}\pi(B-A)^2\rho U. \tag{2}$$

In the case of rotation about the base, with $f(x) = \omega(x-A)$, it gives

$$M = \tfrac{1}{8}\pi\rho\omega(B-A)^3, \tag{3}$$

a result identical with (2) if the 'effective velocity' of the fin is taken as the mean value,

$$U = \tfrac{1}{2}\omega(B-A). \tag{4}$$

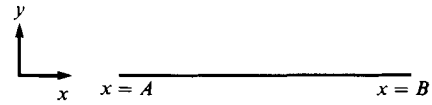

FIGURE 1. Solid strip of width $B-A$, taken as in motion normal to itself (in the y-direction) with velocity $f(x)$.

2. Case of a single fin attached to a body of elliptic cross-section

We now consider the case (relevant to gymnotiform motion) of a single fin attached to a non-moving body, where we specify the body cross-section as an ellipse with major axis $2s$ and minor axis $2t$. The fin (see figure 2) is taken as extending a distance $l-s$ beyond the end of the major axis, so that the fin tip is at a distance l from the centre of the elliptic cross-section.

We study the momentum of the flow resulting from movement of this fin by using a conformal mapping of the external flow field onto the simpler flow field studied in §1. The necessary conformal mapping is achieved in two stages, where an intermediate stage consists of the case of a circular body cross-section with a fin attached to it.

First of all we use the classical mapping

$$x = (r+a^2r^{-1})\cos\theta, \quad y = (r-a^2r^{-1})\sin\theta, \tag{5}$$

applying it not to the entire region outside the circle $r = a$ but only to that part of it which lies outside the larger circle $r = c$ (figure 3). This part is mapped onto the outside of an ellipse

$$x = s\cos\theta, \quad y = t\sin\theta \tag{6}$$

with major and minor axes $2s$ and $2t$ as in figure 2, where

$$s = c+a^2c^{-1}, \quad t = c-a^2c^{-1}. \tag{7}$$

The same mapping converts a fin attached to the circular cross-section along the radius $\theta = 0$ from $r = c$ to $r = h$ (see figure 3) into a fin extending from $x = s$ to $x = l$ beyond the tip of the ellipse's major axis (as in figure 2), where

$$l = h+a^2h^{-1}. \tag{8}$$

Secondly, we use the different conformal mapping

$$X = (r+c^2r^{-1})\cos\theta, \quad Y = (r-c^2r^{-1})\sin\theta \tag{9}$$

to transform the circular cross-section $r = c$ into a flat strip extending from $X = -2c$ to $X = +2c$. The same mapping (see figure 3) transforms the fin $\theta = 0$, $c < r < h$ into an extension of the same strip $Y = 0$ from $X = +2c$ to $X = B$, where

$$B = h+c^2h^{-1}. \tag{10}$$

The two-stage mapping illustrated in figure 3 maps the entire flow field outside the elliptic cross-section of figure 2 onto a simpler flow field outside a strip extending as in figure 1 from $X = A$ to $X = B$, where in this case

$$A = -2c. \tag{11}$$

We note that part of the strip (the part extending from $X = -2c$ to $X = +2c$) corresponds to the body cross-section and is therefore motionless; while the remainder (extending from $X = +2c$ to $X = B$) is subject to movement since it corresponds to the fin.

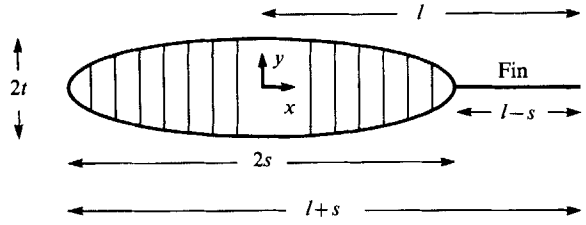

FIGURE 2. Elliptic cross-section of fish body, with major axis $2s$ and minor axis $2t$ and with a fin of width $l-s$ attached. Here, Cartesian coordinates x, y are used. (Note that in this diagram the cross-section, for mathematical convenience, is turned through 90° from its natural position with the fin vertical.)

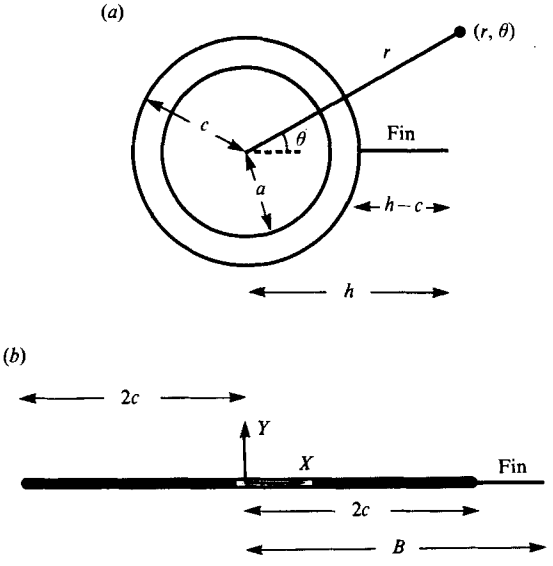

FIGURE 3. (*a*) Circular cross-section of radius c, with a fin of width $h-c$ attached. Here, polar coordinates r, θ are used. (*b*) Solid strip of length $4c$, with a fin of width $B-2c$ attached. Here, Cartesian coordinates X, Y are used.

In the present problem, exactly as in §4 of Part 1 (see equation (6) in particular) we can write the momentum (in the y-direction) per unit length as an integral

$$M = \rho \oint \phi \, \mathrm{d}x \tag{12}$$

in the positive sense around the boundary. We can also show that this momentum M is left unchanged by the above mapping.

To prove this invariance of M we note that the velocity potential ϕ is the real part of a complex potential

$$\phi + \mathrm{i}\psi, \tag{13}$$

where the stream function ψ is zero on the motionless body but non-zero on the moving fin. Accordingly, the form (12) of M as an integral around the entire cross-section can be rewritten as the real part of

$$\rho \oint (\phi + \mathrm{i}\psi)(\mathrm{d}x + \mathrm{i}\,\mathrm{d}y) \tag{14}$$

because $\psi \, \mathrm{d}y$ is zero on the entire boundary (that is, on the body surface where $\psi = 0$ *and* on the fin where $y = 0$). But by Cauchy's theorem this complex integral is

$(2\pi i)$ times the coefficient of $(x+iy)^{-1}$ in the behaviour of $\phi+i\psi$ as $|x+iy|\to\infty$, which cannot be changed by our mappings.

It follows that we can apply the result (1) of §1, with A and B as in (11) and (10), to give

$$M = 2\rho \int_{+2c}^{h+c^2h^{-1}} (\partial\phi/\partial Y)_{Y=0} (X+2c)^{\frac{1}{2}} (h+c^2h^{-1}-X)^{\frac{1}{2}} \, dX. \tag{15}$$

Here, the lower limit for the integral is written $+2c$ instead of $-2c$ because the velocity

$$(\partial\phi/\partial Y)_{Y=0} \tag{16}$$

of the strip is zero in the part $-2c < X < +2c$ corresponding to the body.

We now express the integral (15) as an integral with respect to r along the fin which figure 3 shows attached to the circular cross-section. We take this fin as moving perpendicular to itself with velocity

$$r^{-1}\,\partial\phi/\partial\theta = g(r) \quad (c < r < h). \tag{17}$$

The conformal nature of the mapping implies that

$$(\partial\phi/\partial Y)_{Y=0}\, dX = g(r)\, dr; \tag{18}$$

essentially, the mapping stretches both the X-coordinate and the Y-coordinate 'conformally' – that is, to an equal extent (as can be verified from (9), which give

$$dX = (1-c^2r^{-2})\, dr, \quad dY = (1-c^2r^{-2})\, r\, d\theta \tag{19}$$

on $\theta = 0$). Accordingly, the expression (15) for M becomes

$$\begin{aligned} M &= 2\rho \int_c^h g(r)\,(r+c^2r^{-1}+2c)^{\frac{1}{2}} (h+c^2h^{-1}-r-c^2r^{-1})^{\frac{1}{2}}\, dr \\ &= 2\rho \int_c^h g(r)\,(1+cr^{-1})\,(h-r)^{\frac{1}{2}} (r-c^2h^{-1})^{\frac{1}{2}}\, dr. \end{aligned} \tag{20}$$

We now specialize the discussion to the case when the fin attached to the elliptic cross-section of figure 2 is simply rotating about its base with angular velocity ω. Its velocity normal to itself is then

$$(\partial\phi/\partial y)_{y=0} = \omega(x-s) \quad (s < x <, l). \tag{21}$$

But the mapping (5) converts dy on $y = 0$ into

$$(1-a^2r^{-2})\, r\, d\theta \quad \text{on} \quad \theta = 0. \tag{22}$$

(Compare equation (19) in the case of the other mapping.) The value of $g(r)$ defined by equation (17) is therefore

$$g(r) = (1-a^2r^{-2})\,\omega(x-s) \quad (c < r < h), \tag{23}$$

which equations (5) and (7) allow us to express entirely in terms of r, a and c as

$$g(r) = (1-a^2r^{-2})\,\omega(r+a^2r^{-1}-c-a^2c^{-1}). \tag{24}$$

Substitution of this expression for $g(r)$ in equation (20) gives

$$M = 2\rho\omega \int_c^h (h-r)^{\frac{1}{2}} (r-c^2h^{-1})^{\frac{1}{2}} (r-a^2c^{-1})\,(1-c^2r^{-2})\,(1-a^2r^{-2})\, dr, \tag{25}$$

an integral which we can compute very straightforwardly for a wide range of cases.

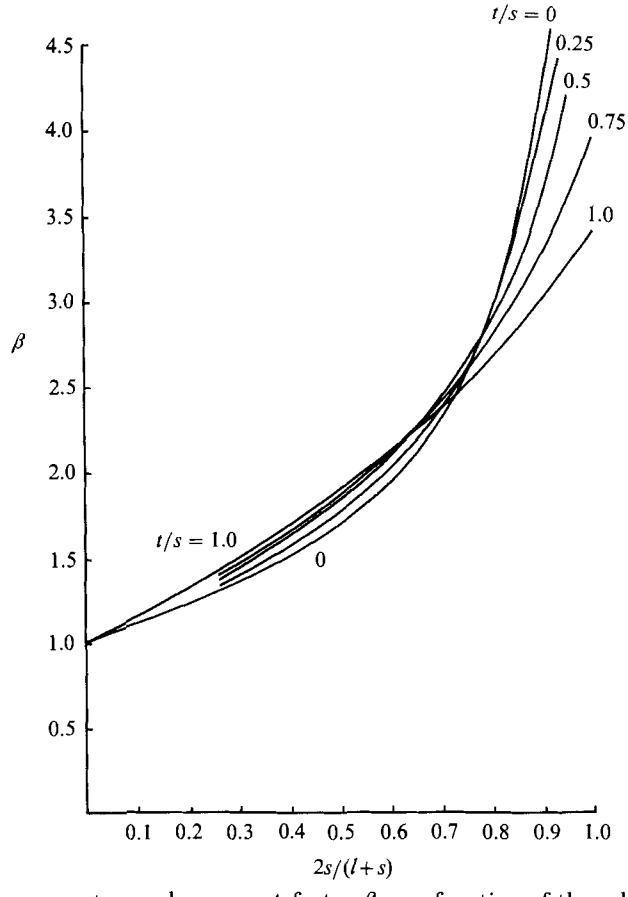

FIGURE 4. The momentum enhancement factor β as a function of the solidity ratio $2s/(l+s)$ (see figure 2) for various axis ratios t/s.

Figures 4 and 5 show the results of these computations. They plot the coefficient β, representing any departure from the case (3) of a fin by itself. Thus we write

$$\beta = M/M_1, \quad \text{where} \quad M_1 = \tfrac{1}{8}\pi\rho\omega(l-s)^3. \tag{26}$$

By equation (3), M_1 represents the fluid momentum associated with motion of the fin of figure 2 in the absence of any body.

For five different ratios

$$t/s = 0, 0.25, 0.5, 0.75, 1.0 \tag{27}$$

of the minor axis to the major axis of the ellipse, figure 4 plots the coefficient β as a function of the ratio

$$2s/(l+s) \tag{28}$$

of body depth $2s$ to the total depth of body and fin $(l+s)$. By contrast, our second figure, 5, plots β as a function of the axis-ratio t/s for ten different values of this 'solidity ratio'

$$2s/(l+s) = 0, 0.1, 0.2, \ldots, 0.9. \tag{29}$$

These figures suggest a significant enhancement of fin added mass due to the presence of a non-moving body. Particularly for larger values of the solidity ratio (that is, when most of the total depth of body and fin is taken up by body) the

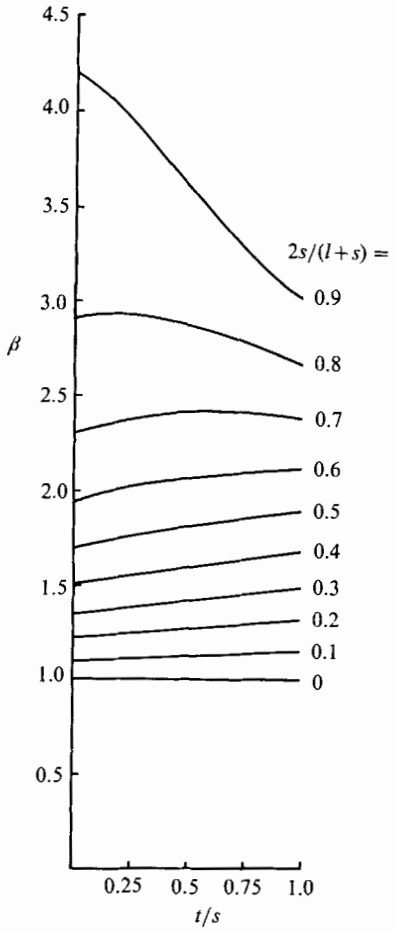

FIGURE 5. The momentum enhancement factor β as a function of the axis ratio t/s for different values of the solidity ratio $2s/(l+s)$.

enhancement factor β can take quite large values, in the region of 3 or 4; or even more as the solidity ratio tends to 1.

In this context it may be of interest to note the limiting behaviour of β as the solidity ratio tends to 1 (case of an extremely small fin). It is easily proved that for any ellipse with non-zero axis-ratio t/s the limiting value of β in this case is

$$\frac{16}{3\pi}\left(1+\frac{s}{t}\right) = 1.70\left(1+\frac{s}{t}\right). \tag{30}$$

This limit gets larger as the axis ratio t/s becomes small. When the case of a completely flat body ($t/s = 0$) is considered, on the other hand, we find that the limiting behaviour of β as the solidity ratio (28) tends to 1 takes the asymptotic form

$$\beta \sim \frac{64}{15\pi}\left(\frac{l+s}{l-s}\right)^{\frac{1}{2}} = 1.36\left(\frac{l+s}{l-s}\right)^{\frac{1}{2}}; \tag{31}$$

an asymptotic form to which the *uppermost* part of the calculated curve for $t/s = 0$ shown in figure 4 does already closely approximate.

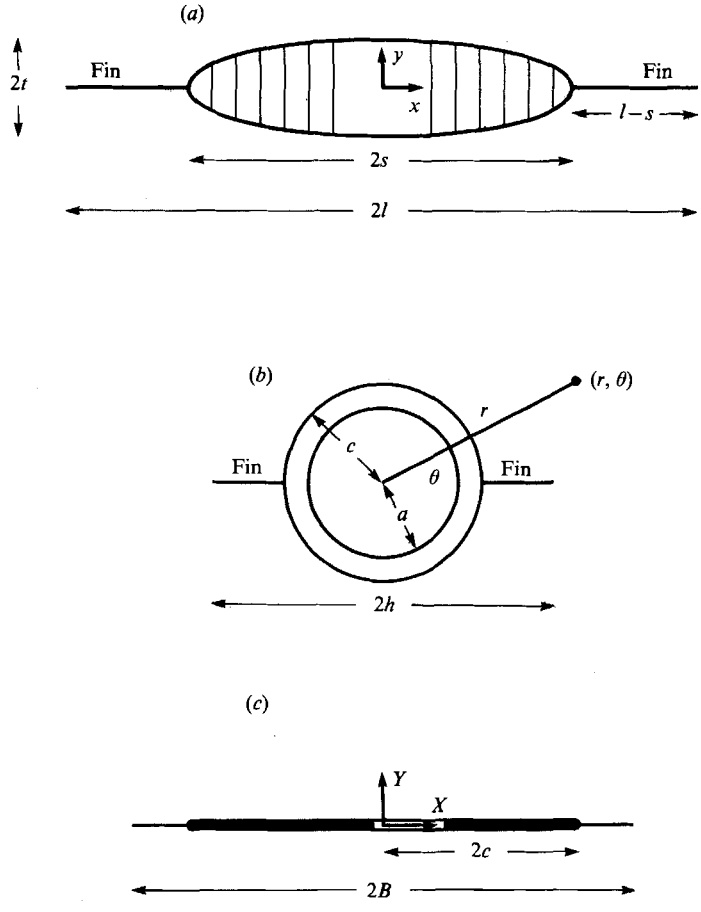

FIGURE 6. (*a*) Elliptic cross-section of fish body, with major axis $2s$ and minor axis $2t$ and with two fins of width $l-s$ attached (Cartesian coordinates x, y). (*b*) Circular cross-section of radius c, with two fins of width $h-c$ attached (polar coordinates r, θ). (*c*) Solid strip of length $4c$, with two fins of width $B-2c$ attached (Cartesian coordinates X, Y).

3. Case of two equal fins attached to a body of elliptic cross-section

We now consider the case (relevant to balistiform locomotion) of two equal fins attached to a non-moving body of which the cross-section is again specified as an ellipse with major axis $2s$ and minor axis $2t$. The fins (see figure 6) are taken as extending an equal distance $l-s$ beyond each end of the major axis, so that each fin tip is at a distance l from the centre of the elliptic cross-section.

We study the momentum of the flow resulting from *symmetric motions* of these two fins by using the same conformal mappings (5) and (9) as in §2. Equation (5) maps the outside of the circular cross-section $r = c$ onto the outside of the ellipse (6). Furthermore, the same mapping converts a pair of fins attached to the circular cross-section along the radii $\theta = 0$ and $\theta = \pi$ from $r = c$ to $r = h$ (see figure 6) into fins extending from $x = s$ to $x = l$ and from $x = -s$ to $x = -l$ beyond the ends of the major axis of the ellipse, where l and h are related by equation (8).

Again, the other conformal mapping (9) transforms the circular cross-section $r = c$ into a flat strip $Y = 0$ extending from $X = -2c$ to $X = +2c$. Furthermore, the same mapping (see figure 6) transforms the fins $c < r < h$, $\theta = 0$ and $\theta = \pi$ into extensions

of the same strip from $X = +2c$ to $X = B$ and from $X = -2c$ to $X = -B$, with B as defined in (10).

Thus the two-stage mapping illustrated in figure 6 maps the entire flow field outside the stationary elliptic cross-section, resulting from symmetric motions of both fins, onto a simpler flow field outside a strip extending as in §1 from $X = A$ to $X = B$, where in this case

$$A = -B. \tag{32}$$

Here we use once again the fact that the momentum per unit length, M, is unchanged by the mapping (see §2) to obtain from expression (1) for M the result

$$M = 2\rho \int_{-B}^{B} (\partial\phi/\partial Y)_{Y=0} (B+X)^{\frac{1}{2}} (B-X)^{\frac{1}{2}} \, \mathrm{d}X. \tag{33}$$

On the other hand, part of the strip (the part extending from $X = -2c$ to $X = +2c$) corresponds to the body cross-section and is therefore motionless. The other two parts (extending from $X = +2c$ to $X = B$ and from $X = -2c$ to $X = -B$) are subject to exactly symmetrical motions because they correspond to the fins. Accordingly, (33) can be written with the integral replaced by exactly twice the integral from $X = 2c$ to $X = B$, as follows:

$$M = 4\rho \int_{2c}^{B} (\partial\phi/\partial Y)_{Y=0} (B^2-X^2)^{\frac{1}{2}} \, \mathrm{d}X. \tag{34}$$

Now we can write this integral in terms of $g(r)$, defined in (17) as the velocity perpendicular to itself of the corresponding fin attached to the circular cross-section and stretching from $r = c$ to $r = h$ along the radius $\theta = 0$ (see either figure 3 or figure 6). Since $g(r)$ once again satisfies (18), the expression (34) for M can be rewritten

$$M = 4\rho \int_{c}^{h} g(r) \, [(h + c^2 h^{-1})^2 - (r + c^2 r^{-1})^2]^{\frac{1}{2}} \, \mathrm{d}r, \tag{35}$$

where (9) and (10) have been used to substitute for X and B.

Next, specializing the discussion to the case when the two fins attached to the elliptic cross-section of figure 6 are simply rotating about their bases with identical angular velocity ω in a symmetrical fashion, we can substitute expression (24) for $g(r)$ in (35). This gives, after some simplification,

$$M = 4\rho\omega \int_{c}^{h} \left(1 - \frac{a^2}{r^2}\right)\left(r - \frac{a^2}{c}\right)\left(1 - \frac{c}{r}\right) \frac{(h^2 r^2 - c^4)^{\frac{1}{2}} (h^2 - r^2)^{\frac{1}{2}}}{hr} \, \mathrm{d}r, \tag{36}$$

an integral which we can compute very straightforwardly for a wide range of cases.

Figures 7 and 8 show the results of these computations. They plot the coefficient β, representing any departure of the momentum M for a pair of fins from twice the momentum in the case (3) of a single fin by itself. Thus we write

$$\beta = M/M_0, \quad \text{where} \quad M_0 = \tfrac{1}{4}\pi\rho\omega(l-s)^3. \tag{37}$$

Here, M_0 represents twice the momentum associated with motion of just one of the fins of figure 6 *in the absence of any body or of the other fin.*

For five different ratios (27) of the minor axis to the major axis of the ellipse, figure 7 plots the coefficient β as a function of the solidity ratio s/l, defined now as the ratio of the body depth $2s$ to the total depth $2l$ of the body and *both* fins. In the limiting case as this solidity ratio s/l tends to 1 (case of a pair of extremely small fins), (30) and (31) once again represent the limiting behaviour of β under conditions of

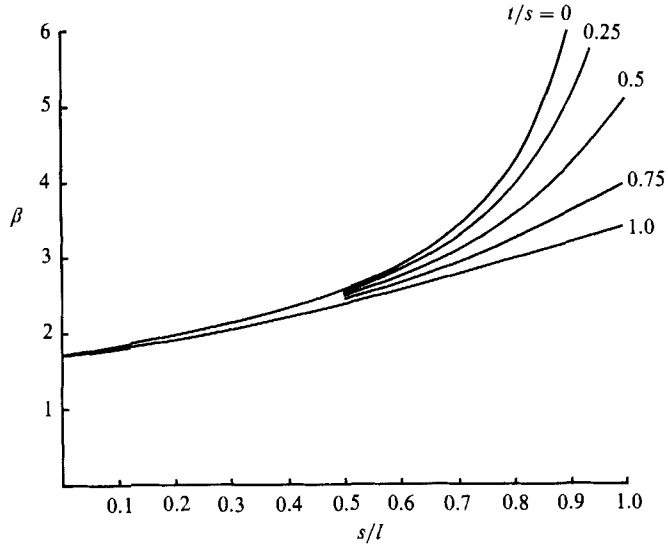

FIGURE 7. Case of two fins. The momentum enhancement factor β as a function of the solidity ratio s/l (see figure 6) for various axis ratios t/s.

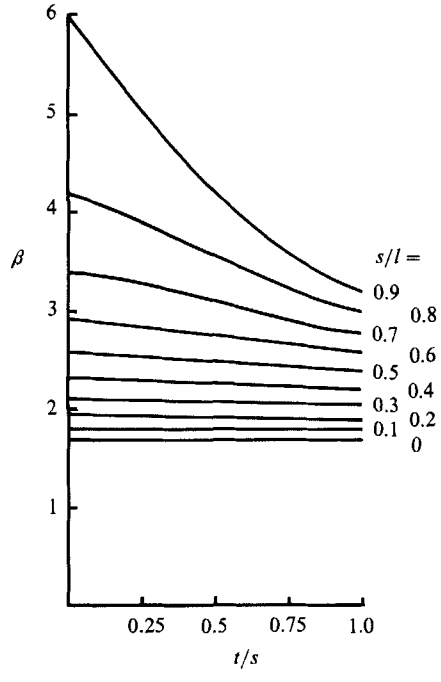

FIGURE 8. Case of two fins. The momentum enhancement factor β as a function of the axis ratio t/s for different values of the solidity ratio s/l.

non-zero axis ratio t/s and zero axis ratio respectively. At lower values of the solidity ratio, however, the momentum enhancement factor β for a pair of fins behaves in a somewhat simpler way than for a single fin – omitting, in fact, the 'crossings-over' characteristic of figure 4.

Again, figure 8 plots β as a function of the axis ratio t/s for ten different values of the solidity ratio,

$$s/l = 0, 0.1, 0.2, \ldots, 0.9. \tag{38}$$

Both figures reconfirm that the momentum enhancement is very substantial for larger values of the solidity ratio. Undulations of small dorsal and ventral fins attached to a deep fish body give, in short, a lot more thrust than would be produced by similar undulations of each of the fins on its own. For the biological significance of this result, see Part 1.

REFERENCE

LIGHTHILL, J. & BLAKE, R. 1990 Biofluiddynamics of balistiform and gymnotiform locomotion. Part 1. Biological background, and analysis by elongated-body theory. *J. Fluid Mech.* **212**, 183–207 (referred to as Part 1).